

Voltage-driven quantum oscillations of conductance in graphene

V. A. Yampol'skii^{1,2}, S. S. Apostolov^{1,2},

Z. A. Maizelis^{1,2}, Alex Levchenko^{1,3}, and Franco Nori^{1,4}

¹ *Advanced Science Institute, The Institute of Physical and Chemical Research (RIKEN),
Wako-shi, Saitama, 351-0198, Japan*

² *A. Ya. Usikov Institute for Radiophysics and Electronics
Ukrainian Academy of Sciences, 61085 Kharkov, Ukraine*

³ *Institute for Theoretical Physics, University of California,
Santa Barbara, California, 93106, USA*

⁴ *Department of Physics, Center for Theoretical Physics,
Applied Physics Program, Center for the Study of Complex Systems,
University of Michigan, Ann Arbor, MI 48109-1040, USA*

(Dated: June 14, 2022)

Abstract

Locally-gated single-layer graphene sheets have unusual discrete energy states inside the potential barrier induced by a finite-width gate. These states are localized outside the Dirac cone of continuum states and are responsible for novel quantum transport phenomena. Specifically, the longitudinal (along the barrier) conductance exhibits oscillations as a function of barrier height and/or width, which are both controlled by a nearby gate. The origin of these oscillations can be traced back to singularities in the density of localized states. These graphene conductance-oscillations resemble the Shubnikov-de-Haas (SdH) magneto-oscillations; however, here these are driven by an electric field instead of a magnetic field.

PACS numbers: 73.63.-b

I. INTRODUCTION

The unusual and rather remarkable transport properties of graphene continue to attract considerable attention. Soon after its experimental discovery¹, studies found: unconventional quantum Hall effect²; the possibility of testing the Klein paradox³; specular Andreev reflection and Josephson effect⁴; new electric field effects^{5,6}; intriguing electron lensing⁷; and other fascinating phenomena (see, e.g., recent papers⁸⁻¹⁶ and references therein). Studies of graphene are also inspired by their potential application in nano-electronic devices, since an applied electric field can vary considerably the electron concentration and have both electrons and holes as charge carriers with high mobility.

The subject of the present study, which is a logical continuation of recent work⁶, is an unusual novel transport effect, namely, *voltage-driven* quantum oscillations in the conductance of a single-layer gated graphene. These oscillations originate from a new type of electron states in graphene. When a graphene sheet is subject to nearby gates, these create an energy barrier for propagating electrons. Here we explicitly demonstrate that, in contrast to non-relativistic quantum mechanics, where localized states can exist only inside quantum wells, Dirac-like *relativistic* electrons in graphene allow energy states localized *within the barrier*. We show that the energy $\varepsilon(q_y)$ of the localized states (versus the wave vector component q_y along the barrier) becomes *non-monotonic* if

$$V_0 D > \pi \hbar v_F,$$

where V_0 and D are the barrier height and width correspondingly, and v_F is the Fermi velocity. This produces singularities in the density of localized states for energies where

$$d\varepsilon/dq_y = 0.$$

When the magnitude and/or width of the barrier changes, the locations of the singularities move and periodically cross the Fermi level, generating quantum oscillations in the *longitudinal* (along the barrier) conductance as well as in the thermodynamic properties of graphene. This situation resembles the well known physical mechanism for Shubnikov-de Haas (SdH) magneto-oscillations (see, e.g., Ref.^{17,18}). Indeed, electrons in the conduction band of a 3D metal subject to a strong magnetic field have an equidistant discrete energy levels (Landau levels) separated by the cyclotron energy. The corresponding density of states

has singularities at the Landau levels. When the magnetic field is changed, the positions of the Landau levels move and pass periodically through the Fermi energy. As a result of this, the population of electrons at the Fermi level also changes periodically, giving rise to the quantum oscillations of both the transport and thermodynamic properties of a metal. One should notice, however, a few important differences. First, in the context of gated graphene, oscillations are induced by the *electric* field, while the corresponding SdH oscillations are driven by a *magnetic* field. Second, localized energy states in graphene are non-equidistant and the resulting density of states has a rather complicated energy dependence. Thus, the corresponding oscillations in the conductance inherit all these unusual peculiarities.

II. LOCALIZED ENERGY STATES IN A BARRIER

The tunneling of relativistic particles in graphene *across* a finite-width potential barrier, and its corresponding conductance, has been recently studied (see, e.g., Refs.^{3,7,19–21}). Here we consider another conduction problem, namely, electron waves that propagate *strictly along* the barrier and *damp away from it*. More specifically, we consider electron states in graphene with a potential barrier located in a single-layer graphene occupying the xy -plane (see Fig. 1). For simplicity, we assume that the barrier $V(x)$ has sharp edges,

$$V(x) = \begin{cases} 0, & |x| > D/2, \\ V_0, & |x| < D/2. \end{cases} \quad (1)$$

Electrons in monolayer graphene obey the Dirac-like equation (hereafter $\hbar = 1$),

$$i\frac{\partial\psi}{\partial t} = \hat{H}\psi, \quad \hat{H} = -iv_F\hat{\boldsymbol{\sigma}} \cdot \nabla + V(x), \quad (2)$$

where $\hat{\boldsymbol{\sigma}} = (\hat{\sigma}_x, \hat{\sigma}_y)$ are the Pauli matrices. We then seek stationary spinor solutions of the form,

$$\psi(x, y) = \psi(x) \exp(-i\varepsilon t + iq_y y), \quad (3)$$

with energy ε and momentum q_y along the barrier. We focus on states with $|q_y| > |\kappa| \equiv |\varepsilon|/v_F$. In this case, the electron waves satisfying Eq. (2) damp away from the barrier, and

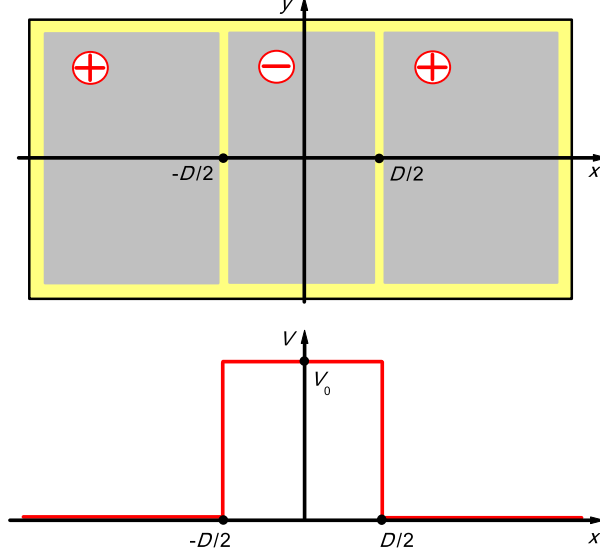


FIG. 1: (Color online) Schematic top view of a graphene sheet (yellow rectangle) placed under voltage gates indicated by the grey block rectangles. Bottom: gate-induced potential energy barrier $V(x)$ in graphene.

the components ψ_1 and ψ_2 of the Dirac spinor can be written in the form

$$\psi_1(x) = \begin{cases} a \exp[k_x(x + D/2)], & x < -D/2, \\ b \exp(iq_x x) \\ \quad + c \exp(-iq_x x), & |x| \leq D/2, \\ d \exp[-k_x(x - D/2)], & x > D/2, \end{cases} \quad (4)$$

$$\psi_2(x) = \begin{cases} a \frac{i\kappa}{k_x + q_y} \exp[k_x(x + D/2)], & x < -D/2, \\ -b \exp(iq_x x + i\theta) \\ \quad + c \exp(-iq_x x - i\theta), & |x| \leq D/2, \\ -d \frac{i\kappa}{k_x - q_y} \exp[-k_x(x - D/2)], & x > D/2, \end{cases} \quad (5)$$

with real $k_x = (q_y^2 - \kappa^2)^{1/2}$ and $q_x = ((\kappa - \mathcal{V}/D)^2 - q_y^2)^{1/2}$. Here $\mathcal{V} = V_0 D / v_F$ is the effective barrier strength and $\tan \theta = q_y / q_x$.

Matching the functions $\psi_1(x)$ and $\psi_2(x)$ at the points $x = \pm D/2$, we obtain a set of four linear homogeneous algebraic equations for the constants a , b , c , and d . Equating the determinant of this set to zero, we obtain a dispersion relation for the localized electron energy states,

$$F(\varepsilon, q_y) \equiv \tan(q_x D) + \frac{k_x q_x}{\kappa(\mathcal{V}/D - \kappa) + q_y^2} = 0. \quad (6)$$

The spectrum of localized states in graphene [Eq. (6)] is shown by the solid black curves in Fig. 2, for dimensionless variables

$$Q = q_y D, \quad \mathcal{E} = \varepsilon D / v_F. \quad (7)$$

This spectrum consists of an infinite number of branches $\mathcal{E}_n(Q)$. Each of these branches starts from the lines $\mathcal{E} = \pm|Q|$ (red solid straight lines in Fig. 2) at

$$\mathcal{E} = \mathcal{V}/2 - \pi^2 n^2 / 2\mathcal{V} \quad (8)$$

and tends asymptotically to the line

$$\mathcal{E} = \mathcal{V} - Q$$

with increasing Q (dashed red line in Fig. 2). Furthermore, a particular branch of the spectrum starts at the point ($Q = 0, \mathcal{E} = 0$) and also tends to the line $\mathcal{E} = \mathcal{V} - Q$.

The behavior of different branches of the spectrum depends on the barrier strength \mathcal{V} . If $\mathcal{V} < \pi/2$, then all branches satisfy $\mathcal{E} < 0$. Localized states with positive energies appear only for $\mathcal{V} > \pi/2$. When \mathcal{V} increases, new branches in the spectrum with positive energies appear. When \mathcal{V} is within the interval

$$(n + 1/2)\pi < \mathcal{V} < (n + 3/2)\pi,$$

the number of branches with $\mathcal{E} > 0$ is $n + 1$, for $n = 1, 2, 3, \dots$. It is worth emphasizing that each of the branches with positive energy has a maximum \mathcal{E}_n^{\max} at a certain wave number $Q = Q_n^{\max}$. Near these points the group velocity of localized electron waves tends to zero, which resembles the stop-light phenomena found in various media²². The localized states can also be observed in graphene when a voltage is applied to produce a potential well²³.

Note that defect-induced localized electron states in graphene and the enhancement of conductivity due to an increase of the electron density of states localized near the graphene edges were recently reported²⁴. In contrast to these examples, the electron states studied here are localized within the barrier and also these *are tunable*, i.e., the energy levels can be shifted by charging the barrier strength (e.g., via tuning a gate voltage).

III. DENSITY OF LOCALIZED STATES

To calculate the density of electron states $\rho(\varepsilon)$, we use the general formula $\rho(\varepsilon) = \sum_{\alpha} \delta(\varepsilon - \varepsilon_{\alpha})$, where the index α labels the quantum state and $\delta(x)$ is Dirac's delta-function. Using

$$\sum_{\alpha} (\dots) = 4L_x L_y (2\pi)^{-2} \int dk_x dk_y (\dots) \quad (9)$$

for a continuum spectrum one finds the already familiar expression

$$\rho_{\text{cont}}(\mathcal{E}) = \rho_0 |\mathcal{E}|, \quad \rho_0 = \frac{2L_x L_y}{\pi v_F D}, \quad (10)$$

where L_x and L_y are the lengths of the graphene sheet in the x and y directions, respectively. For localized energy states, we obtain:

$$\rho_{\text{loc}}(\mathcal{E}) = 2\rho_0 \frac{D}{L_x} \sum_n \left| \frac{d\mathcal{E}_n(Q)}{dQ} \right|_{\mathcal{E}_n(Q)=\mathcal{E}}^{-1}, \quad (11)$$

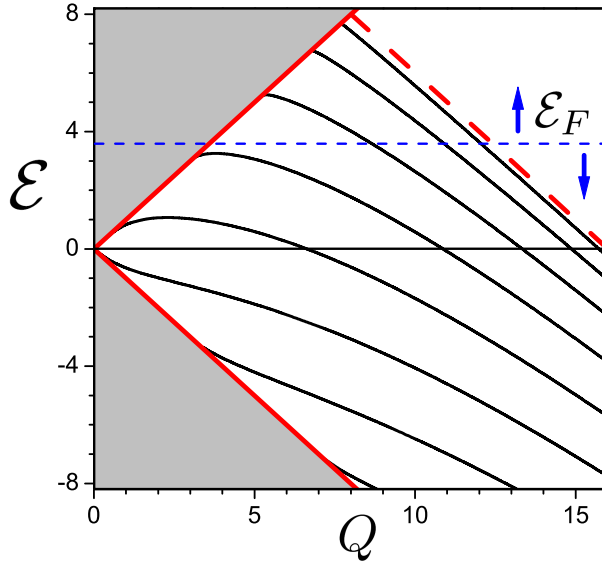


FIG. 2: (Color online) Electron energy spectrum in graphene obtained for positive Q and $\mathcal{V} = 16$. The Dirac sea of delocalized states (continuum spectrum) is marked by the grey regions. The branches of the spectrum for *localized* states are shown by solid black curves between the straight solid and dashed red lines. There are no states in the forbidden (white) regions. The increase or decrease (schematically indicated by the upward and downward vertical blue arrows) of the Fermi level \mathcal{E}_F (marked by the horizontal dashed blue line) results in a periodic change in both the density of states at $\mathcal{E} = \mathcal{E}_F$, and also in the conductance.

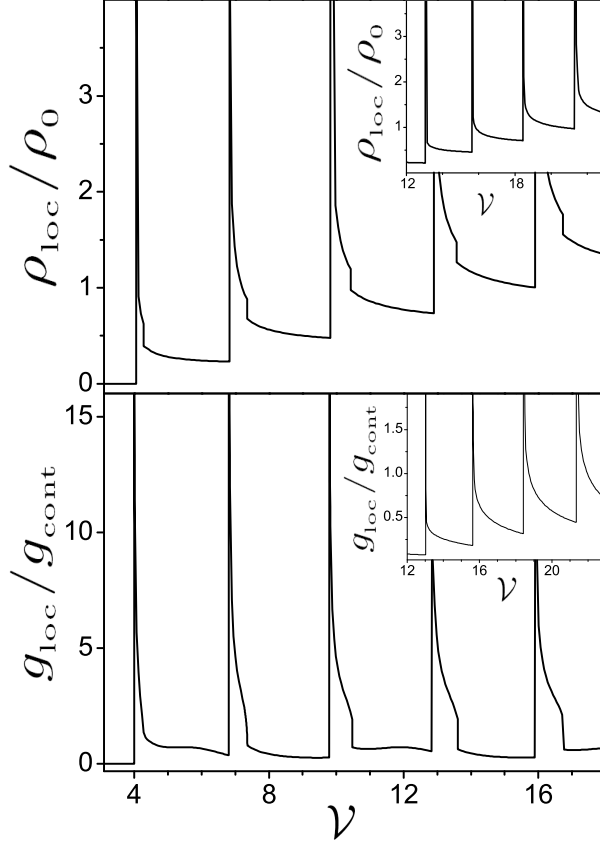


FIG. 3: Dimensionless oscillating parts of the density of states ρ_{loc}/ρ_0 at the Fermi level (upper panel) and conductance $g_{\text{loc}}/g_{\text{cont}}$ (lower panel) versus the strength \mathcal{V} of the potential barrier for $D/L_x = 0.1$, $\mathcal{E}_F = 1$ (main panels) and $\mathcal{E}_F = 5$ (insets). The total conductance is $g = g_{\text{cont}} + g_{\text{loc}}$.

where n runs over the positive roots of the equation $\mathcal{E}(Q) = \mathcal{E}$. The function $\rho_{\text{loc}}(\mathcal{E})$ exhibits two types of peculiarities. First, increasing \mathcal{E} , the jumps or steps (each of magnitude $2D/L_x$) in $\rho_{\text{loc}}(\mathcal{E})/\rho_0$ occur at the points, given by Eq. (8), where new branches of the spectrum arise or disappear. More importantly, *singularities* are observed when $\mathcal{E} = \mathcal{E}_n^{\text{max}}$, where $|\text{d}\mathcal{E}/\text{d}Q|^{-1}$ in Eq. (11) diverges.

The locations of the singularities *shift* when changing the barrier strength \mathcal{V} . Therefore, they periodically cross the Fermi level \mathcal{E}_F . This produces quantum oscillations in the density of states at the Fermi energy, which are seen in the upper panel of Fig. 3, showing $\rho_{\text{loc}}(\mathcal{E})/\rho_0$ versus the effective barrier strength \mathcal{V} .

IV. KUBO FORMULA AND CONDUCTANCE

A. Kubo expression for the conductance in graphene

When studying transport, within linear response theory, one usually starts from the current-response function,

$$K_{\mu\nu}(\mathbf{x}, \mathbf{x}') = -i\vartheta(t - t')\text{Tr} \left\{ \hat{\rho} [\hat{\mathbf{j}}_{\mu}^H(\mathbf{x}), \hat{\mathbf{j}}_{\nu}^H(\mathbf{x}')] \right\}, \quad (12)$$

where $\mathbf{x} = (\mathbf{r}, t)$, $\vartheta(t)$ is the Heaviside step-function, $\hat{\rho}$ is the equilibrium density matrix, and

$$\hat{\mathbf{j}}_{\mu}^H(\mathbf{r}, t) = \exp(i\hat{H}t)\hat{\mathbf{j}}_{\mu}(\mathbf{r})\exp(-i\hat{H}t)$$

is the current operator in the Heisenberg representation with the Hamiltonian taken from Eq. (2), and where $[\dots, \dots]$ stands for the commutator. For electrons with a linear Dirac spectrum, one finds

$$\hat{\mathbf{j}}_{\mu}(\mathbf{r}) = ev_F\hat{\psi}^{\dagger}(\mathbf{r})\hat{\sigma}_{\mu}\hat{\psi}(\mathbf{r}). \quad (13)$$

Equation (12) is used to define the frequency-dependent linear conductance as

$$g_{\mu\nu}(\omega) = \Re \frac{i}{\omega L_{\mu}L_{\nu}} \iint d\mathbf{r} d\mathbf{r}' K_{\mu\nu}(\mathbf{r}, \mathbf{r}'; \omega). \quad (14)$$

Here \Re stands for the real part of a complex number.

We expand the fermionic field operator $\hat{\psi}(\mathbf{r}, t)$ in terms of exact eigenfunctions [Eq. (3)], namely,

$$\hat{\psi}(\mathbf{r}, t) = \sum_{\alpha} \psi_{\alpha}(\mathbf{r}) \exp(-i\epsilon_{\alpha}t\hat{a}_{\alpha}), \quad (15)$$

and then perform quantum averaging in Eq. (12) with the help of Wick's theorem and the relation $\text{Tr}\{\hat{\rho}\hat{a}_{\alpha}^{\dagger}\hat{a}_{\beta}\} = \delta_{\alpha\beta}f(\epsilon_{\alpha})$, where

$$f(\epsilon) = 1/[\exp[(\epsilon - \epsilon_F)/T] + 1]$$

is the Fermi occupation function. Performing a Fourier transform and using

$$\Re[i/(\epsilon - \epsilon' + \omega + i0)] = \pi\delta(\epsilon - \epsilon' + \omega) \quad (16)$$

Eq. (14), reduces to

$$g_{\mu\nu}(\omega) = \frac{\pi(ev_F)^2}{L_{\mu}L_{\nu}} \int_{-\infty}^{+\infty} d\epsilon \frac{f(\epsilon_+) - f(\epsilon_-)}{\omega} \times \text{Tr} \left\{ \hat{\sigma}_{\mu}\delta(\epsilon_+ - \hat{H})_{\mathbf{r}\mathbf{r}'}\hat{\sigma}_{\nu}\delta(\epsilon_- - \hat{H})_{\mathbf{r}'\mathbf{r}} \right\}, \quad (17)$$

where $\varepsilon_{\pm} = \varepsilon \pm \omega/2$ and the trace incorporates spatial integrations. The operator delta-functions can be directly related to the single-particle Green's functions

$$\hat{G}_{\varepsilon}(\mathbf{r}, \mathbf{r}') = \langle \mathbf{r} | (\varepsilon - \hat{H})^{-1} | \mathbf{r}' \rangle$$

according to

$$\delta(\varepsilon - \hat{H})_{\mathbf{r}\mathbf{r}'} = \frac{1}{2\pi i} [\hat{G}_{\varepsilon}^a(\mathbf{r}, \mathbf{r}') - \hat{G}_{\varepsilon}^r(\mathbf{r}, \mathbf{r}')], \quad (18)$$

where the superscript a/r stands for the advanced/retarded component, respectively. As a result, one finds for the conductance

$$g_{\mu\nu}(\omega) = \frac{(e\nu_F)^2}{4\pi L_{\mu}L_{\nu}} \int_{-\infty}^{+\infty} d\varepsilon \frac{f(\varepsilon_+) - f(\varepsilon_-)}{\omega} \times \text{Tr} \left\{ \hat{\sigma}_{\mu} [\hat{G}_{\varepsilon_+}^a(\mathbf{r}, \mathbf{r}') - \hat{G}_{\varepsilon_+}^r(\mathbf{r}, \mathbf{r}')] \hat{\sigma}_{\nu} [\hat{G}_{\varepsilon_-}^r(\mathbf{r}', \mathbf{r}) - \hat{G}_{\varepsilon_-}^a(\mathbf{r}', \mathbf{r})] \right\}. \quad (19)$$

Next we incorporate disorder by introducing the one-particle scattering time τ , for Dirac fermions, into the Green's function,

$$\langle \hat{G}_{\varepsilon}^{r/a} \rangle_{\text{dis}} \approx (\varepsilon - \hat{H} \pm i/\tau)^{-1}, \quad (20)$$

which enters through the imaginary-part of the corresponding self-energy. The subindex “dis” refers to disorder. Furthermore, we factorize the average of the product of two Green's functions by the product of their averages,

$$\langle \hat{G}_{\varepsilon_+}^r \hat{G}_{\varepsilon_-}^a \rangle_{\text{dis}} \approx \langle \hat{G}_{\varepsilon_+}^r \rangle_{\text{dis}} \langle \hat{G}_{\varepsilon_-}^a \rangle_{\text{dis}}. \quad (21)$$

This assumption should be valid for weak disorder and together with Eq. (20) is equivalent to the self-consistent Born approximation.

B. Conductance along the barrier

We now focus on the *along-the-barrier* ($\mu = \nu = y$) conductance for the geometry shown in Fig. 1. At zero temperature, $T \rightarrow 0$, when $f(\varepsilon) = \vartheta(\varepsilon_F - \varepsilon)$ and the ε integration is bounded by the frequency ω , for the average dc-conductance $g \equiv \langle g_{yy}(\omega \rightarrow 0) \rangle_{\text{dis}}$ we find (per spin and per valley):

$$g = g_{\text{cont}} + g_{\text{loc}}. \quad (22)$$

The first contribution g_{cont} here comes from the extended electron energy states with corresponding density of states taken from Eq. (10), and reads explicitly (now keeping \hbar) as

$$g_{\text{cont}} = \frac{\pi e^2 L_x}{16\hbar L_y} \left[\varepsilon_F \tau + \frac{1}{\pi} \left(1 - \varepsilon_F \tau \arctan \frac{1}{\varepsilon_F \tau} \right) \right]. \quad (23)$$

At the neutrality point, $\varepsilon_F = 0$, from Eq. (23) one recovers a universal (i.e., scattering time τ -independent) result $g_{\text{cont}} = \sigma_{\text{min}}(L_x/L_y)$, where $\sigma_{\text{min}} = (\pi/8)(e^2/h)$ is the minimal conductivity, which received considerable attention in a number of recent studies (e.g., Refs.^{20,25}).

Away from the neutrality point, the conductance grows linearly with the Fermi energy,

$$g_{\text{cont}} = (\pi e^2/16\hbar)(L_x/L_y)\varepsilon_F \tau. \quad (24)$$

The novel result of the present study is the *oscillatory* part g_{loc} , which originates from the electron states localized within the barrier. It can be expressed, with the help of Eq. (11), as follows:

$$g_{\text{loc}} = \frac{2e^2 D}{\hbar L_y} \sum_n \int_0^\infty d\mathcal{E} \left| \frac{dQ}{d\mathcal{E}_n} \right|_{\mathcal{E}_n=\mathcal{E}} \frac{M(\mathcal{E})\eta^2}{[(\mathcal{E} - \mathcal{E}_F)^2 + \eta^2]^2}, \quad (25)$$

where

$$M(\mathcal{E}) = \left| \int \frac{dx}{D} \psi_\alpha^*(x) \hat{\sigma}_y \psi_\alpha(x) \right|^2$$

is the matrix element constructed from the wave-functions of localized states, Eq. (4)-(5), and $\eta = D/v_F \tau$. The remaining integration in Eq. (25) is simplified realizing that everywhere away from the integrable square-root singularities of $|dQ/d\mathcal{E}_n|$, the η -dependent function is peaked at the Fermi energy, whereas $M(\mathcal{E})$ is smooth. Thus, one finally finds,

$$\frac{g_{\text{loc}}(\mathcal{V}, \mathcal{E}_F)}{g_{\text{cont}}} = \frac{16 D}{\mathcal{E}_F L_x} M(\mathcal{E}_F) \sum_n \left| \frac{dQ}{d\mathcal{E}_n} \right|_{\mathcal{E}_n=\mathcal{E}_F}, \quad (26)$$

where the conductance g_{loc} is normalized to its continuous part taken away from the neutrality point, namely, where $g_{\text{cont}} \propto \tau \varepsilon_F$. Note that

$$\mathcal{E}_F = \varepsilon_F \frac{D}{v_F}.$$

The derivative entering Eq. (26) can be calculated with the help of the dispersion equation (6) as $(dQ/d\mathcal{E}) = -(dF/d\mathcal{E})/(dF/dQ)$, and reads

$$\frac{dQ}{d\mathcal{E}} = Q \frac{\mathcal{V} - 2\mathcal{E} + (\mathcal{V} - \mathcal{E})\sqrt{Q^2 - \mathcal{E}^2}}{(\mathcal{V} - \mathcal{E})\mathcal{E} - Q^2 - Q^2\sqrt{Q^2 - \mathcal{E}^2}}. \quad (27)$$

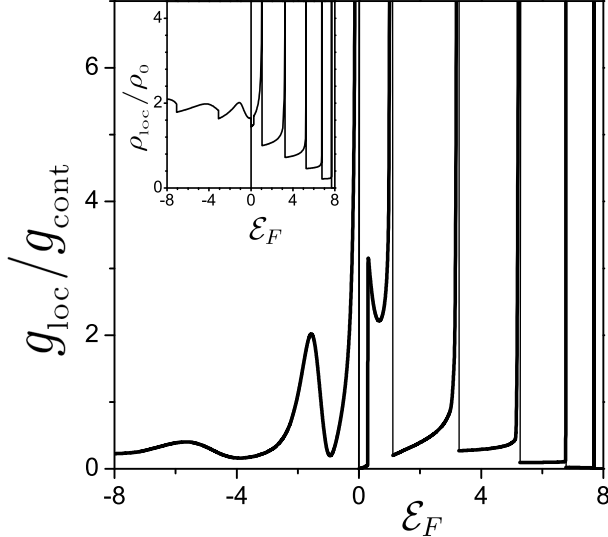


FIG. 4: Dimensionless oscillating parts of the density of states ρ_{loc}/ρ_0 at the Fermi level (inset) and conductance $g_{\text{loc}}/g_{\text{cont}}$ (main panel) versus the Fermi energy \mathcal{E}_F , for $D/L_x = 0.1$, and $\mathcal{V} = 16$.

The oscillatory nature of $g_{\text{loc}}(\mathcal{V}, \mathcal{E}_F)$ is illustrated in the lower panel of Fig. 3. The essential observation, which follows from Eq. (26), is that the longitudinal conductance traces the peculiarities in the density of localized states and opens a direct way for their experimental observation. It is also worth mentioning that close to the singularity of $dQ/d\mathcal{E}$, meaning $|\mathcal{E}_n - \mathcal{E}_F| \lesssim \eta$, the conductance correction is regularized by the finite width of the η -Lorentzian under the integral of Eq. (25).

Varying the concentration of free particles with constant barrier strength, one can again observe oscillations in the density of states (see the inset of Fig. 4). Thus, the part of the conductance originated from the localized states, also oscillates with the change of the Fermi energy (see main panel of Fig. 4).

V. CONCLUSIONS

In summary, we predict a novel type of conductance oscillations in locally-gated single-layer graphene, which are related to the unusual electron states localized within a potential barrier. When the barrier height and/or width is varied, localized levels periodically cross the Fermi energy, inducing modulations in the density of states. The latter translates into unusual quantum oscillations of the conductance. These electric-field-driven quantum oscillations are similar to the Shubnikov-de-Haas oscillations which are produced in metals and

semiconductors when changing the external magnetic field.

Acknowledgments

We gratefully acknowledge partial support from the National Security Agency (NSA), Laboratory of Physical Sciences (LPS), Army Research Office (ARO), National Science Foundation (NSF) grant No. EIA-0130383, JSPS-RFBR 06-02-91200, and Core-to-Core (CTC) program supported by Japan Society for Promotion of Science (JSPS). A.L. acknowledges partial support from the National Science Foundation under Grant No. NSF PHY05-51164.

-
- ¹ K. S. Novoselov, *et. al.*, Science **306**, 666 (2004).
 - ² K. S. Novoselov, *et. al.*, Nature **438**, 197 (2005); Y. Zhang, *et. al.*, Nature **438**, 201 (2005).
 - ³ M. I. Katsnelson, K. S. Novoselov, and A. K. Geim, Nat. Phys. **2**, 620 (2006).
 - ⁴ C. W. J. Beenakker, Phys. Rev. Lett. **97**, 067007 (2006); M. Titov, and C. W. J. Beenakker, Phys. Rev. B **74**, 041401(R) (2006).
 - ⁵ V. Lukose, R. Shankar, and G. Baskaran, Phys. Rev. Lett. **98**, 116802 (2007).
 - ⁶ V. A. Yampol'skii, S. Savel'ev, F. Nori, New J. of Phys. **10**, 053024 (2008).
 - ⁷ V. V. Cheianov, V. Fal'ko, and B. L. Altshuler, Science **315**, 1252 (2007).
 - ⁸ V. P. Gusynin, S. G. Sharapov, J. P. Carbotte, Int. J. Mod. Phys. B **21**, 4611-4658 (2007).
 - ⁹ A. K. Geim, and K. S. Novoselov, Nature Materials **6**, 183 (2007).
 - ¹⁰ C. W. J. Beenakker, Rev. Mod. Phys. **80**, 1337 (2008).
 - ¹¹ A. H. Castro Neto, F. Guinea, N. M. R. Peres, K. S. Novoselov, and A. K. Geim, Rev. Mod. Phys. **81**, 109 (2009).
 - ¹² J. R. Williams, L. DiCarlo, C. M. Marcus, Science **317**, 638 (2007).
 - ¹³ L. DiCarlo, J. R. Williams, Y. Zhang, D. T. McClure, C. M. Marcus, Phys. Rev. Lett. **100**, 156801 (2008).
 - ¹⁴ M. M. Fogler, D. S. Novikov, L. I. Glazman, and B. I. Shklovskii, Phys. Rev. B **77**, 075420 (2008).
 - ¹⁵ Yu. P. Bliokh, V. Freilikher, S. Savel'ev, and F. Nori, Phys. Rev. B **79**, 075123 (2009).

- ¹⁶ A. V. Rozhkov, S. Savel'ev, and F. Nori, arXiv:0808.1636, Phys. Rev. B (to be published).
- ¹⁷ D. Shoenberg, *Magnetic Oscillations in Metals* (Cambridge University Press, Cambridge, 1984).
- ¹⁸ V. P. Gusynin, S. G. Sharapov, Phys. Rev. Lett. **95**, 146801 (2005).
- ¹⁹ H. G. Winful, M. Ngom, and N. M. Litchinitser, Phys. Rev. A **70**, 052112 (2004).
- ²⁰ J. Tworzydło, *et. al.*, Phys. Rev. Lett. **96**, 246802 (2006).
- ²¹ P. G. Silvestrov, K. B. Efetov, Phys. Rev. Lett. **98**, 016802 (2007).
- ²² L. V. Hau, *et. al.*, Nature **397**, 594 (2004); S. Savel'ev, *et. al.*, Nature **2**, 521 (2006).
- ²³ J. M. Pereira, V. Mlinar, F. M. Peeters, and P. Vasilopoulos, Phys. Rev. B **74**, 045424 (2006).
- ²⁴ S. Y. Zhou, *et. al.*, Nature **2**, 595 (2006); S. Banerjee, *et. al.*, Appl. Phys. Lett. **88**, 602111 (2006); A. H. Castro Neto, F. Guinea, N. M. R. Peres, Phys. Rev. B **73**, 205408 (2006).
- ²⁵ M. I. Katsnelson, Eur. Phys. J. B **51**, 157 (2006); J. Cserti, Phys. Rev. B **75**, 033405 (2007); K. Ziegler, Phys. Rev. B **75**, 233407 (2007); K. Nomura, and A. H. MacDonald, Phys. Rev. Lett. **98**, 076602 (2007)